

Effect of hydrostatic pressure on the electrical conductance of polycrystalline magnesite (MgCO_3)

A. N. Papathanassiou

University of Athens, Department of Physics, Section of Solid State Physics, Panepistimiopolis, GR 157 84 Zografos, Athens, Greece
(Received 4 September 1997; revised manuscript received 23 February 1998)

The room-temperature conductance of polycrystalline magnesite was measured, for different hydrostatic pressures up to 3 kbar. The electrical conductivity decreases with increasing pressure, indicating that the conductivity mechanism is dominantly ionic. The $\ln G(P)$ plots are curved and obey a second-order polynomial law. The curvature is interpreted, in the usual manner, either in terms of a pressure-dependent activation volume model or by asserting that the pressure activates additional conduction modes. Additionally, a theoretical $\ln G(P)$ equation was derived, by assuming that the activation volume is not single valued, but follows a Gaussian distribution function. The three models were employed to analyze the experimental data and estimate the activation volume for the conduction mechanism. The analyses provided compatible zero-pressure values of the activation volume. The results are discussed in relation to those reported for dolomite. [S0163-1829(98)01931-6]

I. INTRODUCTION

Calcite (CaCO_3), magnesite (MgCO_3) and their mixed crystal dolomite [$\text{CaMg}(\text{CO}_3)_2$] constitute the calcite family, which is the most well known and representative group among the carbonate salts. The calcite group members share the rhombohedral crystal structure, which is also called the calcite structure.¹⁻³ There are potential differences between the calcite group members and the typical ionic crystals, such as sodium chloride:¹ The structural units of a simple ionic material are single cations and anions, which are ionically bonded; the carbonate matrix consists of cations and a trioxycarbon radical. The Cl ions have a spherical symmetry in the simple NaCl structure and serve as centres of symmetry. This is not the case for the carbonates; the carbonate radical forms an equilateral triangle, with the oxygens located at the edges and the carbon placed in the center.^{1,4} Although the calcite group crystals are classified as ionic materials, they exhibit the feature that the bonding inside the carbonate is covalent whereas, as recently found for magnesite,⁴ the bonding between the cation and the carbonate is strongly ionic, with a small but significant covalent contribution. The specific crystal structural and bonding peculiarities, which the calcite-type crystals exhibit in comparison to the features of simple ionic crystals, render them interesting materials for pure, theoretical and experimental, study. Moreover, the calcite-type crystals constitute a proper, complete set of materials for working on the field of mixed crystals, as magnesite and calcite are the end members of the mixed crystal dolomite.

A systematic investigation of the dielectric and electrical properties of the calcite family have been conducted recently.⁵⁻¹¹ In those papers, we studied the effect of mixing on the defect structure establishment and on the dipole dynamic. The free charge transport phenomena were also studied through dielectric relaxation experiments.

Magnesite is itself a challenging system for transport experiments, since covalent bonding exists in a dominantly

ionic matrix. Besides, the collection of the values of the activation volume for the mixed crystal and its compounds is desirable, for understanding the influence of the lattice constant variation (long-range effect¹²) and the modification of the environment (the structural units), which surrounds the transferring charge carrier, to the value of the activation volume. We have already reported the results for dolomite,⁹ while, in the present paper, we study the conductivity phenomena under pressure in magnesite. Apart from the interest in the pure research on carbonate salts, our results may contribute to more advantageous technological applications,¹³ since carbonates are widely used in the industry for preparing refractory materials, cements, paper, rubber, and pharmaceutical products. Recalling that the calcite-type materials are widespread earth materials, our results may also be used for the microscopic interpretation of long-range electrical geophysical phenomena.^{14,15}

II. THEORY

The transport experiments under pressure provide information for the identity of the conduction mechanism and probe the volume changes induced by the formation, migration and association of defects.¹⁶ Concerning the transport phenomena, pressure studies may define the origin of the transport mechanism; i.e., whether an ionic, electronic or protonic mechanism operates.^{17,18} Besides, the effect of pressure is quantitatively described through the evaluation of the activation volume v^{act} .

For the ionic crystals, the conductance measurements in the vicinity of room temperature (RT) usually determine the activation volume v^{act} in the association region, through the following equation:^{16,19-22}

$$v^{\text{act}} = -kT \left[\left(\frac{\partial \ln G}{\partial P} \right)_T - \gamma \kappa_0 \right], \quad (1)$$

where k denotes the Boltzmann's constant, G is the sample's conductance, γ is the Grüneisen constant, and κ_0 is the iso-

thermal compressibility of the matrix. Provided that the term $\gamma\kappa_0$ is practically negligible, the following simplified approximate equation is valid:

$$v^{\text{act}} \cong -kT \left(\frac{\partial \ln G}{\partial P} \right)_T. \quad (2)$$

The significance of the $\gamma\kappa_0$ term for the analysis of the rough experimental data, will be discussed in detail in Sec. IV. There is no physical argument that imposes the activation volume to be pressure independent.¹⁴ The percentage variation of the activation volume v^{act} with respect to pressure is expressed by the compressibility κ^{act} of the activation volume:¹⁴

$$\kappa^{\text{act}} = -\frac{1}{v^{\text{act}}} \left(\frac{\partial v^{\text{act}}}{\partial P} \right)_T. \quad (3)$$

If we assume that κ^{act} holds a constant nonzero value and that $|\kappa^{\text{act}}P| \ll 1$, an analytical approximate expression for the conductance as a second-order polynomial of pressure can be derived:¹⁴

$$\ln \left(\frac{G(P)}{G(0)} \right) = \left[\frac{v^{\text{act}}(0)}{kT} - \gamma\kappa_0 \right] P - \left[\frac{\kappa^{\text{act}} v^{\text{act}}(0)}{2kT} \right] P^2, \quad (4)$$

where we have labeled the ambient pressure as zero pressure and we assumed the quantities κ_0 and γ are constant.

Modified theory of the ionic conductivity under pressure. It has long been known that the activation energy E^{act} of the conductivity mechanism in many insulators is not single valued, but it follows a distribution function.²³ For the calcite,⁶ dolomite,¹⁰ and magnesite,²⁴ we found that the activation energy for long-distance charge transport is distributed. Depending on the specific type of material, the activation energy E^{act} can be either directly identified to the migration enthalpy h^m for the transfer of free charge carriers, or, most likely, it can be regarded as a sum of the migration enthalpy plus a portion of association energy E^{ass} for the formation of defect dipoles (i.e., impurity-vacancy agglomerates).^{25,26} If the association energy is presumed, in the latter case, as single valued, we may state that the distribution in the activation energy results somehow from the distribution of the migration enthalpy. Thus, the distribution in the activation energy is assigned to the spatial variation of the height of the potential barriers. It is reasonable to assume that the activation energy values for the conduction mechanism accumulate around a central value. It is convenient to consider that the distribution around the central value is Gaussian, as it occurs for the bound defect motion.²⁷⁻²⁹

Consider now the simplified picture for the activation volume as being the volume change, when we take two states of the transport process: a ground state and an excited one.¹⁸ The volume change depends on the size of the transferring charge. Now, assume that a certain type of ion migrates through a crystal environment, where the potentials are spatially modified. When the moving charge is instantly located at a saddle point higher than another one, then, the volume change should be larger than that caused when the same carrier is located at a lower saddle point. Hence, the activation volume values are expected to be *not* single valued. Subsequently, the distribution in the activation energy values

results in the distribution in the activation volume values. To a first approximation, the Gaussian distribution in the activation energy is assigned to the modification of the potential barriers. It seems reasonable to consider that the activation volume values follow the Gaussian distribution function:

$$f(v^{\text{act}}) = \frac{1}{\sqrt{2\pi}\sigma} \exp\left(-\frac{(v^{\text{act}} - v_0^{\text{act}})^2}{2\sigma^2}\right) \quad (5)$$

where v_0^{act} is the central value and σ is the broadening parameter. According to Eq. (2), the conductance decreases exponentially as pressure increases, for a simple mechanism that is characterized by a constant activation volume:

$$G(P)/G(0) = \exp\left(-\frac{v^{\text{act}}}{kT} P\right). \quad (6)$$

The last equation can be modified to include the effect of the distribution in the values of the activation volume:

$$\begin{aligned} \frac{G(P)}{G(0)} &= \int_{-\infty}^{+\infty} f(v^{\text{act}}) \frac{G(P, v^{\text{act}})}{G(0, v^{\text{act}})} dv^{\text{act}} \\ &= \int_{-\infty}^{+\infty} \frac{1}{\sqrt{2\pi}\sigma} \exp\left(-\frac{(v^{\text{act}} - v_0^{\text{act}})^2}{2\sigma^2}\right) \\ &\quad \times \exp\left(-\frac{v^{\text{act}}}{kT} P\right) dv^{\text{act}}. \end{aligned} \quad (7)$$

The integral appearing in Eq. (7) is rather a routine one.³⁰ So, Eq. (7) becomes

$$\frac{G(P)}{G(0)} = \exp\left(\frac{\sigma^2}{2} \left(\frac{P}{kT}\right)^2 - v_0^{\text{act}} \left(\frac{P}{kT}\right)\right). \quad (8)$$

By taking the logarithm of the latter relation, we get

$$\ln \left(\frac{G(P)}{G(0)} \right) = \left(\frac{\sigma^2}{2(kT)^2} \right) P^2 - \left(\frac{v_0^{\text{act}}}{kT} \right) P. \quad (9)$$

We conclude that a conduction mechanism, with Gaussian distribution in the activation volume values, provides curved $\ln G(P)$ plots, which obey a second order polynomial law. A second-order polynomial fit to the experimental data directs readily to the evaluation of the central value v_0^{act} and the width parameter σ .

Modified equations, which include a distribution function for the activation energy, have been proposed in order to fit the thermal depolarization curves of insulators.^{27,28,31} A great number of distinguished papers have established, both theoretically and experimentally, that the relaxation mechanisms traced by the thermally stimulated depolarization current (TSDC) experiments, are characterized by the Gaussian distribution in the activation energy, in most cases. To the best of our knowledge, the idea of a distribution of the defect volume parameters has not been worked out yet.

III. EXPERIMENTAL DETAILS

Both the single crystal and the polycrystalline MgCO_3 salts share the name of magnesite. Our samples come from the large deposits of compact polycrystalline magnesite,

which are located in the island of Euboea (Greece).² Their exhibiting characteristic is the white (snowlike) color. This material is known in the literature with the specific name leukolite, which is interpreted as "white-stone," when translated in Greek. The analysis performed by the Institute of Geological and Mining Research (IGME) (Greece), gave the following results: 47.90 % wt MgO, 2.80 % wt Si, 0.02 % wt Al, 0.13 wt % Fe, 0.41 % wt Ca, 0.02 % wt Mn, 0.02 % wt Sr, less than 0.01 % wt K, 0.04 wt % Na and 0.31 % wt humidity.

The experiments were performed in a piston type pressure vessel, which employs oil as the pressure transmitting fluid. The conductance measurements were obtained by a Boonton 75c bridge. The typical dimensions of the specimens were approximately 0.5 mm×4 cm². An extensive description of the pressure apparatus and the details concerning the experimental procedure, have been reported in a paper that appeared recently.⁹

IV. RESULTS AND DISCUSSION

Electrical characterization of the conduction mechanism.

Since the pressure vessel accommodates a two-electrode sample holder,⁹ we checked if the conductance is masked by the probable space-charge contribution: In the working frequency of 5 kHz, we carried out successive measurements at certain constant pressure values, throughout the pressure range. We concluded that the conductivity is within the experimental errors, time independent. The latter investigation is highly desirable when unknown materials are electrically studied; it has been reported that the space-charge contribution is present in rocks, even at a frequency of 1 kHz.³² Moreover, the conductance is actually frequency dependent, but its decrease upon pressure stems from the reduction of the dc conductivity. Thus, the pressure derivative of the conductance directs to the evaluation of the activation volume, indeed, at least for the low-pressure region (See Refs. 33 and 9). Finally, the pressurization cycle is not accompanied by any hysteresis phenomenon. A decrease of the conductance upon pressure is typical for ionic materials and can be interpreted as the reduction of the mobility of the moving species on pressure. The conduction mechanism is impeded, as the increase of the pressure brings the structural units of the material close together. We do not observe even the slightest increase of the conductance upon pressure. Consequently, there does not exist any obvious electronic conduction mechanism,²⁰ neither do traces of humidity detected in the sample's analyses, introduce a protonic-type conductivity.¹⁸ In the past years, curved plots were reported for some ionic crystals,^{34,19} as well as for dolomite.⁹

Quantitative analyses.

In the following, we deal with a couple of pressure experiments: the first was performed at $T = 300$ K and the second one was carried out by cooling the pressure vessel at $T = 290$ K. In Fig. 1, we present the logarithm of the conductance G versus pressure, at $T = 300$ K. The experimental points indicate the nonlinear decrease of the $\ln G(P)$ plot. Within the ionic conductivity model, the curvature in the conductance plot shares three interpretations:

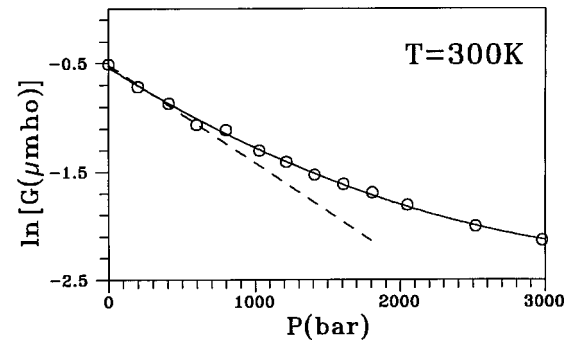


FIG. 1. A typical $\ln G(P)$ plot for polycrystalline magnesite. The solid line is the second-order polynomial curve that best fits the experimental data points. The dashed line is the straight line that fits the low-pressure conductance data.

(i) One or more additional mechanisms become activated, as pressure increases and, consequently, the $\ln G(P)$ plot departs from linearity. Consequently, the slope provides the apparent activation volume value, for each pressure value. In the low-pressure limit, we may obtain the actual (real) activation volume value that corresponds to the zero-pressure state. By fitting the linear Eq. (2) to the data points up to about 650 bar, we get $v^{\text{act}} = (22 \pm 1)$ cm³/mole, at $T = 300$ K and $v^{\text{act}} = (21 \pm 2)$ cm³/mole, at $T = 290$ K. We note that the latter constant values of the activation volume correspond to the low-pressure (zero-pressure) mechanism.

(ii) A unique mode of migration operates and the activation volume is pressure dependent. So, the slope of the conductance plot, at any pressure, gives the value of $v^{\text{act}}(P)$. The percentage variation of the activation volume is expressed through the compressibility κ^{act} , which is defined via Eq. (3). The analytical second-order approximation of Eq. (4) presumes that the compressibility of the activation volume κ^{act} is constant and $|\kappa^{\text{act}}P| \ll 1$. However, we tried a polynomial fit, and found that a second-order polynomial equation best fits the experimental points

$$\ln G(P) = \ln G(0) + aP + bP^2. \quad (10)$$

Using Eqs. (2) and (3), we may prove readily that

$$v^{\text{act}} \cong -kT(a + 2bP), \quad (11)$$

$$\kappa^{\text{act}} = -2b/(a + 2bP). \quad (12)$$

In Table I we present the coefficients a and b , which were derived by fitting Eq. (10) to the experimental data points. Additionally, the zero-pressure value of the activation volume and its compressibility, which were obtained through Eqs. (11) and (12), are depicted. We stress that Eq. (10) results from a pure mathematical procedure, in contrast to Eq. (4), which is derived on the basis of physical arguments ($\kappa^{\text{act}} = \text{constant}$ and $|\kappa^{\text{act}}P| \ll 1$). We point out that a second-order polynomial equation has also been selected in order to analyze the conductivity plots of polymers.³⁵ Varotsos and Alexopoulos proposed that the ratio $\kappa^{\text{act}}/\kappa_0$, where κ_0 is the matrix compressibility should be at most equal to 5.¹⁴ This can serve as an index for checking the quality of the analysis employed. The ratio $\kappa^{\text{act}}/\kappa_0$, where κ_0 is the compressibility of the matrix magnesite, is about 290, at $T = 290$ K and 415, at 300 K. (A detailed discussion on the elastic properties and the compressibility data of polycrystalline magnesite are

TABLE I. Results obtained by the second-order polynomial fit to the relative conductance data. a and b denote the polynomial coefficients of Eq. (10). Following the notation used in the text, model (ii) assumes that a unique conductivity mechanism operates, with pressure-dependent activation volume. The zero-pressure values of $v_0^{\text{act}}(0)$ and $\kappa^{\text{act}}(0)$ were derived via Eqs. (11) and (12). Model (iii) asserts that the activation volume is not single valued, but obeys a Gaussian distribution. v_0^{act} is the central value and σ denotes the broadening parameter.

T (K)	Model (ii)				Model (iii)	
	a (10^{-4} bar $^{-1}$)	b (10^{-7} bar $^{-2}$)	$v_0^{\text{act}}(0)$ (cm 3 /mole)	$\kappa^{\text{act}}(0)$ (GPa $^{-1}$)	v_0^{act} (cm 3 /mole)	$\frac{\sigma}{v_0^{\text{act}}}$
290	-7.98 ± 0.45	1.34 ± 0.14	19 ± 1	3.4 ± 0.4	19 ± 1	0.65 ± 0.04
300	-8.36 ± 0.41	2.04 ± 0.24	21 ± 1	4.9 ± 0.6	21 ± 1	0.76 ± 0.06

given in the next subsection.) These values are about two orders of magnitude larger than those theoretically predicted,¹⁴ but they are comparable to the large experimental values reported for some ionic crystals, like erbium-doped SrF $_2$ (Ref. 36) and sodium doped CaF $_2$.³⁷

(iii) A unique mechanism, which is characterized by a distribution in the values of the activation volume, operates. For a Gaussian distribution, a second-order polynomial fit to the data provides the set of parameters v_0^{act} and σ . Keeping the notation of Eq. (9), we get, in combination with Eq. (10),

$$v_0^{\text{act}} = -akT, \quad (13)$$

$$\sigma = \sqrt{2bkT}. \quad (14)$$

In Table I, we present the central value v_0^{act} and the ratio σ/v_0^{act} , which were obtained by using Eq. (13) and (14). The physical content of assumption (ii) is potentially different than that of assumption (iii): The activation volumes derived from assumption (ii), are zero-pressure ones. On the contrary, v_0^{act} is a mean activation volume and is pressure independent.

The activation volume values, which were obtained by linear fit to the low-pressure data, are compatible, within the experimental errors, to the zero-pressure ones, which were derived from the second-order polynomial fit. They are also in agreement with those obtained when adopting the Gaussian distribution model. The three different ways which were used to analyse the experimental data, provide comparable results and they certify the reliability of the zero-pressure v_0^{act} values. Which of the above models best describes the curved conductivity plots is still an open question. Unfortunately, there is not any experimental scheme that provides a firm answer to the aforementioned question. The common point,

which the three models share, is that they all point to identical zero pressure and the v_0^{act} values for the activation volume, and these values of the activation volume are actually real (not apparent) ones.

The role of the sample's volume change upon pressure.

The activation volume value is usually considered proportional to the $\ln G(P)$ plot, as implied by the approximate Eq. (2). The condition that the term $\gamma\kappa_0$ of Eq. (1) is considerably small is necessary, so as to determine whether a correction to the activation volume values reported above is desired.^{16,18}

How should the conductance data under pressure be analyzed when the specimen is a porous one? Which is the role of the porosity reduction? We have recently proposed a new model³⁸ that provides the elastic term correction to the activation volume evaluation:

$$\left(\frac{\partial \ln G(P)}{\partial P} \right)_T = -\frac{v_0^{\text{act}}}{kT} + \left(\gamma - \frac{2}{3} \right) \kappa_0(P) + \frac{2}{3} \kappa(P) \quad (15)$$

where κ_0 is the compressibility of the solid grains (which are usually labeled as the ‘‘matrix’’ material) and it is certainly identical to the compressibility measured for a single crystal). κ is the compressibility of the polycrystalline material, i.e., the system consisting of the solid frame (matrix) and the intergranular porosity.

The compressibilities appearing in Eq. (15) were obtained from the bulk modulus (which is the inverse of the compressibility) versus the pressure data, for two different samples of dry polycrystalline magnesite.³⁹ We considered that the adiabatic bulk modulus data practically coincide to the isothermal ones. Since, for the majority of the geomate-

TABLE II. Comparative presentation of the RT compressibility κ_0 of the matrix material, the compressibility κ of the polycrystalline material, and the right-hand-side elastic terms appearing in Eq. (15), in relation to the zero-pressure pressure derivative of the $\ln G(P)$ plot. The compressibilities were estimated by exploiting two sets of data cited in Ref. 39, in the way explained in the text. The Grüneisen constant was set equal to 1.7.¹⁴ All data correspond to ambient (zero) pressure.

$\kappa_0(0)$ (GPa $^{-1}$)	$\kappa(0)$ (GPa $^{-1}$)	$(\gamma - \frac{2}{3})\kappa_0(0)$ (GPa $^{-1}$)	$\frac{2}{3}\kappa(0)$ (GPa $^{-1}$)	$-(\partial \ln G(0)/\partial P)_T$ (GPa $^{-1}$)	
				$T=290$ K	$T=300$ K
0.0122	0.0134	0.0126	0.0089	7.98	8.36
0.0126	0.0145	0.0129	0.0097		

rials, the difference between the isothermal elastic data and the adiabatic ones, ranges from 0.5 to 1.3 %, at room temperature.⁴⁰ At ambient pressure, the value of the bulk modulus directs to the (ambient pressure) $\kappa \equiv 1/B$. A linear extrapolation of the high-pressure data, where porosity is reduced, to the zero pressure⁴¹ yields an estimated value of the ambient pressure compressibility $\kappa_0 \equiv 1/B_0$. We estimated two sets of elastic quantities, corresponding to two experimental data sets cited in Ref. 39: $B \equiv 74.6$ GPa, $B_0 \equiv 81.74$ GPa, $dB_0/dP \equiv 8.4$ and $B \equiv 68.9$ GPa, and $B_0 \equiv 74.41$ GPa, $dB_0/dP \equiv 8.4$. Note that the dB_0/dP values (for the matrix material) are compatible to those reported for many ionic materials.¹⁴

In Table II we present the zero-pressure compressibilities $\kappa_0(0)$ and $\kappa(0)$, the elastic terms participating in Eq. (15) and the zero-pressure conductance derivatives. We see that the both elastic terms are (in total) 0.24–0.30 % smaller than the slope $-(\partial \ln G/\partial P)_T$. Consequently, the approximate relation represented by Eq. (2), is excellent. The effects of the matrix material compression and the contribution of the porosity modification do not, practically speaking, influence the activation volume values for magnesite.

Comparison with the results for dolomite [$\text{CaMg}(\text{CO}_3)_2$].

Recently, we measured the conductance of dolomite at RT, for various pressure values up to 3 kbar.⁹ Throughout the pressure range, the conductance plots of both magnesite and dolomite are quite similar; the logarithm of the conductance decreases nonlinearly upon pressure and obeys a second-order polynomial law. In both cases, the conductance is dominantly ionic, with apparent activation volume, which decreases upon pressure. Figure 2 shows the RT zero-pressure activation volume values obtained by linear regression to the low-pressure region, in relation to the unitary cell volume, for magnesite and dolomite. The activation volumes for magnesite and dolomite are close together. It seems that the two systems share the same type of conduction mechanism. We speculate that the size of the transferring ions and the migrating paths are probably the same. A direct inspection on Fig. 2 implies that the activation volume decreases slightly on increasing the unitary cell volume of the carbonate salt. A small unitary volume imposes a large activation volume value. This can be regarded as the strong lattice expansion, which occurs during the operation of the activation mechanism.

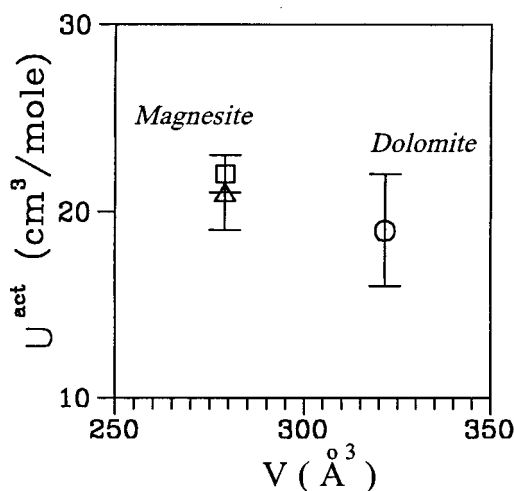


FIG. 2. The room-temperature and zero-pressure activation volumes v^{act} for the calcite-type carbonate salts. Δ , magnesite ($T = 300$ K); \square , magnesite ($T = 290$ K); \circ : dolomite ($T = 294$ K). The results for magnesite are given in the text, while those for dolomite were published previously.⁹

V. CONCLUSION

By varying the pressure, we found that the transport phenomena of polycrystalline magnesite are described, at room temperature, by the ionic conductivity model. The conduction mechanism is imbedded throughout the pressure range (up to 3 kbar). The logarithm of the conductance decreases nonlinearly upon pressure. A second-order polynomial line best fits the experimental data points. The curvature in the conductance plots are interpreted through three models: (i) different additional mechanisms are activated as pressure augments, (ii) a unique mechanism with activation volume, which is pressure dependent, operates, or (iii) the activation volume is not single valued, but follows a Gaussian distribution function around a central value. The data were analyzed by using each of the above-mentioned models. The activation volume values, which were evaluated via the three models, are mutually compatible. The comparison of the present results to those reported for dolomite, indicates that the activation volume for the calcite-type carbonate salts, decreases slightly upon the volume of the hexagonal unit cell.

¹R. J. Reeder, *Crystal Chemistry of Rhombohedral Carbonates*, in *Reviews in Mineralogy*, Vol. 11, Carbonates: Mineralogy and Chemistry, edited by R. J. Reeder (Mineralogical Society of America, Washington, 1983).

²M. H. Battey, *Mineralogy for Students* (Longman, London, 1981).

³W. A. Deer, R. A. Howie, and J. Zussman, *An Introduction to the Rock Forming Minerals* (Longman, Essex, 1966).

⁴M. Catti, A. Pavese, R. Dovesi, and V. R. Saunders, *Phys. Rev. B* **47**, 9189 (1993).

⁵J. F. de Lima, E. M. Yoshimura, and E. Okuno in *Thermoluminescence and Ionic Thermocurrent in Calcite*, International Con-

ference on Defects in Insulating Materials ICDIM88 (Parma, Italy, 1988).

⁶N. G. Bogris, J. Grammatikakis, and A. N. Papathanassiou *Proceedings of the XII International Conference on Defects in Insulating Materials ICDIM92, Germany, 1992*, edited by O. Kanert and J.-M. Spaeth (World Scientific, Singapore, 1993), p. 804.

⁷A. N. Papathanassiou, J. Grammatikakis, V. Katsika, and A. B. Vassilikou-Dova, *Radiat. Eff. Defects Solids* **134**, 247 (1995).

⁸A. N. Papathanassiou and J. Grammatikakis, *Phys. Rev. B* **53**, 16 252 (1996).

⁹A. N. Papathanassiou and J. Grammatikakis, *Phys. Rev. B* **53**, 16 247 (1996).

- ¹⁰A. N. Papathanassiou and J. Grammatikakis, *J. Phys. Chem. Solids* **58**, 2107 (1997).
- ¹¹A. N. Papathanassiou and J. Grammatikakis, *Phys. Rev. B* **56**, 8590 (1997).
- ¹²R. Robert, R. Barboza, G. F. L. Ferreira, and M. Ferreira de Souza, *Phys. Status Solidi B* **59**, 335 (1973).
- ¹³A. Baysar and J. L. Kuester, *IEEE Trans. Microwave Theory Tech.* **40**, 2108 (1992).
- ¹⁴P. A. Varotsos and K. D. Alexopoulos, *Thermodynamics of Point Defects and Their Relation with Bulk Properties*, edited by S. Amelinckx, R. Gevers, and J. Nihoul (North-Holland, Amsterdam, 1985).
- ¹⁵J.-P. Poirier, *Europhys. News* **25**, 25 (1994).
- ¹⁶G. A. Samara, *J. Phys. Chem. Solids* **40**, 509 (1979).
- ¹⁷Hoang-The-Giam, Ai Bui, P. Destruel, and M. Saidi, *J. Phys. (Paris), Colloq.* **C8**, 217 (1984).
- ¹⁸J. J. Fontanella *et al.*, *Macromolecules* **29**, 4944 (1996).
- ¹⁹B.-E. Mellander and D. Lazarus, *Phys. Rev. B* **29**, 2148 (1984).
- ²⁰D. R. Figueroa, J. J. Fontanella, M. C. Wintersgill, and C. G. Andeen, *Phys. Rev. B* **29**, 5909 (1984).
- ²¹G. A. Samara, *Phys. Rev. Lett.* **44**, 670 (1980).
- ²²W. H. Taylor, W. B. Daniels, B. S. H. Royce, and R. Smoluchowski, *J. Phys. Chem. Solids* **27**, 39 (1966).
- ²³J. Vanderschueren and J. Gasiot, *Field Induced Thermally Stimulated Currents in Thermally Stimulated Relaxation in Solids*, edited by P. Braünlich (Springer-Verlag, Berlin, 1979).
- ²⁴A. N. Papathanassiou, Ph.D. Dissertation, University of Athens, 1995.
- ²⁵Wang Da Yu and A. S. Nowick, *Phys. Status Solidi A* **73**, 165 (1982).
- ²⁶I. Kunze and P. Müller, *Phys. Status Solidi A* **13**, 197 (1972).
- ²⁷W. van Weperen and H. W. den Hartog, *Phys. Rev. B* **18**, 2857 (1978).
- ²⁸E. Laredo, M. Puma, N. Suarez, and D. R. Figueroa, *Phys. Rev. B* **23**, 3009 (1981).
- ²⁹J. P. Calame, J. J. Fontanella, M. C. Wintersgill, and C. Andeen, *J. Appl. Phys.* **58**, 2811 (1985).
- ³⁰See the tabulated integral No. 15.75 in M. R. Spiegel, *Mathematical Handbook of Formulas and Tables (Schaum's Outline Series)*, (McGraw-Hill, New York, 1968).
- ³¹W. van Weperen, B. P. M. Lenting, E. J. Bijvank, and H. W. den Hartog, *Phys. Rev. B* **16**, 2953 (1977).
- ³²D. A. Lockner and J. Byerlee, *J. Geophys. Res.* **90**, 7837 (1985).
- ³³C. Bridges and A. V. Chadwick, *Solid State Ionics* **28-30**, 965 (1988).
- ³⁴P. C. Allen and D. Lazarus, *Phys. Rev. B* **17**, 1913 (1978).
- ³⁵J. J. Fontanella *et al.*, *Macromolecules* **29**, 4944 (1996).
- ³⁶C. Andeen, L. M. Hayden, and J. Fontanella, *Phys. Rev. B* **21**, 794 (1980).
- ³⁷J. J. Fontanella, M. C. Wintersgill, and C. G. Andeen, *Phys. Status Solidi B* **97**, 303 (1980).
- ³⁸A. N. Papathanassiou, *J. Phys. Chem. Solids* **58**, 2107 (1997).
- ³⁹*Numerical Data and Functional Relationships in Science and Technology*, Landolt-Börnstein New Series Group V, Vol. 1, Pt. b, edited by G. Angenheister (Springer-Verlag, Berlin, 1982), pp. 57–58.
- ⁴⁰*Numerical Data and Functional Relationships in Science and Technology* (Ref. 39), p. 5.
- ⁴¹Chi-Yuen Wang, *J. Geophys. Res.* **79**, 771 (1974).